Voltage Dependence of Na Channel Blockage by Amiloride: Relaxation Effects in Admittance Spectra

Jens Warncke and Bernd Lindemann

2nd Department of Physiology, Universität des Saarlandes, 6650 Homburg/Saar, Federal Republic of Germany

Summary. Amiloride, present in the mucosal solution, causes the appearance of a distinct additional dispersion in the admittance spectrum of the apical membrane of toad urinary bladder. The parameters of this dispersion (characteristic frequency, amplitude) change with amiloride concentration and with membrane voltage. They allow the calculation of the overall rate constants for Na channel blockage by the positively charged form of amiloride, and the voltage dependence of these rate constants. The on-rate of blockage increases and the off-rate decreases when the membrane surface to which cationic amiloride has access, is made more positive. This result is suggestive of a blocking model where the cationic amidino group of amiloride, depending on its charge, senses 10 to 13% of the membrane voltage while invading the channel entrance by a single-step process, and rests at an electrical distance corresponding to 24 to 30% of membrane voltage while occupying the blocking position.

Key Words   amiloride · relaxation · admittance · current-voltage curves · epithelial Na channels · toad urinary bladder

Introduction

In studies of epithelial transport, impedance or admittance spectra have often been used to assay resistance and capacitance of the apical and basolateral membrane [e.g., 7, 13, 17, 18, 35]. With two membranes of different properties in series the spectra should contain one dispersion for each of them, i.e. two time constants. However, the spectra often contain more than two dispersions. In some instances the additional dispersions were interpreted as effects arising in the solution space outside of the membranes [13]. In other cases they may indicate the presence of voltage-dependent conductances or voltage-dependent channel blockage, as is well known from other membrane systems [26, 38].

We show that the presence of amiloride in the mucosal solution generates a distinct additional dispersion in the admittance spectrum of the apical membrane. From the concentration and voltage dependence of dispersion parameters the overall rate constants of Na channel blockage by the charged form of amiloride may be calculated.

Our results were in part reported at the 1985 spring meeting of the Deutsche Physiologische Gesellschaft [40].

Materials and Methods

Toads (*Bufo marinus*, Mexican origin) were obtained from Lemberger Assoc. (Wisconsin) and kept unfed at room temperature with access to tap water. After double-pithing, the urinary bladder was removed, stretched and mounted with the serosa backed by a filter paper on a Lucite® ring of 3 cm² free window area. The ring was then inserted between two Lucite half-chambers. A hydrostatic pressure of 10 cm water column was applied continuously on the mucosal side, pressing the tissue gently against the filter paper in order to reduce microphonics in the current records. Between the Lucite mounting surface and the apical side of the epithelium an undercured silicon washer was inserted to achieve good sealing with minimal mechanical force and to minimize edge damage.

The urinary bladders were depolarized with a serosal KCl-sucrose solution [31] for more than one hour before measurements. This solution was also used during the experiment. With K-depolarized basolateral membranes the cellular voltage is expected to be close to the serosal voltage (for a discussion *see* [12, 23]). The mucosal medium was a Na_2SO_4 solution of 60 mM Na activity (activity coefficient 0.55, *see* [12]). It contained 1 mM $CaSO_4$, amiloride of 0.15 to 4.8 μM as indicated and was buffered with 3.15 mM K-phosphate at pH 5.5. All solutions were used at room temperature. During recordings aeration of the serosal solution was continued but perfusion of the mucosal half-chamber either lowered to about 1 ml/min, or stopped.

The chamber was placed onto a shock-mounted table within a large Faraday's cage. The transepithelial voltage (V) was controlled by a newly designed low-noise voltage clamp, using bipolar amplifiers of low-input voltage noise and low bias current as voltage sensors (OP 27 GZ, PMI). A low current noise, ultra-low bias current FET-input operational amplifier of switchable gain (AD 515, Analog Devices) was used for current-to-voltage conversion. Command voltages were generated by computer. All digital lines connecting the computer to the interface were optocoupled and interface and clamp were run on a separately

grounded power supply to remove computer-generated interference from the command signals. Current was sampled under program-control with a 12 bit A/D converter. Current flowing from the mucosal solution into the cells will be designated as positive. In consequence voltages positive on the mucosal side with respect to the serosal side of the epithelium are positive.

After completing a voltage pattern at a given submaximal blocker concentration, the protocol was repeated in the presence of 30 or 80 μM amiloride, i.e. while the apical Na channels were completely blocked, to obtain the shunt resistance R_p (Fig. 1A) and the shunt current. The latter was subtracted from the total current recorded before, yielding the amiloride-blockable Na current, I_{Na}. Notably the retrieval of relaxation time constants from the current records did not require this subtraction, but it was essential for the evaluation of amplitude information.

The advantage of sinusoidal voltage perturbation, apart from the implicit Laplace transformation of the data, is the in principle high frequency resolution. Furthermore, drift correction can easily be applied, and the influence of equivalent circuit elements in series to the apical membrane can be removed by appropriate stripping of the spectra. Holding voltages between -40 and $+140$ mV were applied to the clamp and superimposed with sinusoidal voltages of 8 to 2 mV amplitude (depending on frequency), generated digitally and stored in a ROM. Sinewave frequencies (f) were automatically decreased from 1600 to 0.23 Hz (4 steps per octave) with 16 to 2 periods recorded at each f [39]. The sinusoidal current response was amplified and sampled in synchrony with the ROM readout. When the lowest f was 0.23 Hz, data aquisition for one set of sinewaves took 130 sec. For each frequency the current time course was drift-corrected, averaged and evaluated for amplitude and phase.

The resulting impedance spectra were analyzed in terms of coefficients of complex rational functions as described by H. Strobel [37]. This method has a larger range of convergence than conventional least-squares regression. The polynomial coefficients were rearranged into equations which could be solved for parameters of equivalent circuits appropriate for epithelia (e.g. Fig. 1A), including the relaxation circuit which represents the blocking kinetics to be studied (Fig. 3B). It will be appreciated that the membrane resistance values obtained by impedance analysis are *slope resistances* and that the membrane conductances obtained by admittance analysis are *slope conductances*. To judge the goodness of fit, the *total mean error* was calculated as the sum of relative residuals of the impedance divided by the number of frequencies (data points) used.

The low frequency dispersion representing the blocking kinetics was then isolated by subtracting the spectrum of the capacitive component from the total admittance spectrum. Once the parameters of the relaxation circuit were known, the admittance spectrum of the relaxation process was reanalyzed by nonlinear least-squares regression in order to obtain the 95% confidence limits of its fit parameters.

For data fitting the iterative descent subroutine package FMFP (FORTRAN) for nonlinear least-squares regression was used. This program is based on the Davidon-Fletcher-Powell algorithm [10] and was written and kindly provided by Dr. Martin Pring, Philadelphia. It returns 95% confidence limits for the parameters retrieved, which were passed on to the subsequent fitting procedures in order to calculate weight factors and to estimate confidence or standard deviations of the final results. Weight factors of individual data points were calculated as

$$W_i = C_i^2 \Big/ \sum_{j=1}^{n} C_j^2$$

where C_i is the 95% confidence limit of the i-th point and n the number of points.

Unless stated otherwise, values reported are means ± 1 SD (standard deviation), i.e., $\pm 73\%$ confidence limits. Values in brackets are 95% confidence limits obtained by nonlinear least-squares regression. In linear regression of Gauss-distributed data the 95% limit is twice as large as the 73% limit.

Semiempirical calculations of the molecular structure of amiloride and of the charge distribution on this molecule were done with the program MINDO/3 (modified intermediate neglect of differential overlap (e.g. [6]). The standard program was kindly provided by Dr. W. Thiel, Wupperthal. Dr. H. Dürr and Mrs. C. Dorweiler, Saarbrücken, adapted it locally to a Siemens 7561. Mrs. Dorweiler programmed the molecule and analyzed the structure suggested by MINDO/3.

Theory

We shall base our analysis on a two-state blocking model previously used for noise analysis of apical Na channels [e.g. 19, 21, 24]. It may be viewed as a reaction scheme of minimal complexity and specifies just two global rate constants, k_{on} and k_{off}, which describe how frequently amiloride of a given concentration will block a channel and how long the block will last. But, contrary to previous derivations, we allow for a voltage dependence of these rate constants. With P designating the probability that a channel is conducting (not blocked), the reaction rate equation will be

$$dP/dt = -k_{on}(V) \cdot A_o \cdot P + k_{off}(V) \cdot (1 - P). \quad (1)$$

By rearrangement we obtain

$$dP/dt = \lambda(V) \cdot (\overline{P}(V) - P) \quad (1a)$$

where

$$\overline{P}(V) = (1 + A_o/K_A(V))^{-1} \quad (2)$$

is the equilibrium value of P at a given voltage,

$$K_A(V) = k_{off}(V)/k_{on}(V) \quad (3)$$

the apparent dissociation constant of the amiloride-receptor complex and

$$\lambda(V) = k_{on}(V) \cdot A_o + k_{off}(V) = k_{off}(V)/\overline{P}(V) \quad (4)$$

the relaxation rate constant. We shall consider small excursions ΔV around the holding voltage V_H such that

$$V = V_H + \Delta V. \quad (5)$$

Then Eq. (1a) may be developed in a Taylor series

(*compare* [15, 26]). Neglection of higher-order terms yields

$$dP/dt = \lambda \cdot (d\bar{P}/dV - dP/dV) \cdot \Delta V. \tag{1b}$$

Note that $d\bar{P}/dV$ is a constant at any V_H. By differentiation with respect to V and with

$$d/dV(dP/dt) = d/dt(dP/dV)$$

(*compare* [15]) we obtain

$$d/dt(dP/dV) = \lambda \cdot (d\bar{P}/dV - dP/dV). \tag{1c}$$

The Laplace transform is

$$(dP/dV)^* = (1/(1 + s/\lambda)) \cdot d\bar{P}/dV \tag{1d}$$

where the star denotes a transform (complex amplitude) and the initial condition has been set to zero for periodic disturbances.

The *current* flowing through an ensemble of apical Na channels will be

$$I_{Na} = I_0(V) \cdot P(V) \tag{6}$$

where I_0 is the value in the absence of amiloride (i.e. when $P = 1$). I_0 is expected to increase monotonically and instantaneously with V [12, 16, 31]. With Eq. (5) and $\Delta V = 0$ we obtain

$$\bar{I} = \bar{I}_0(V_H) \cdot \bar{P}(V_H) = \bar{I}_0(V_H) \cdot k_{\text{off}}(V_H)/2(V_H). \tag{6a}$$

For $\Delta V \neq 0$ Eq. (6) is developed in a Taylor series such that $\bar{I}$ and V_H are the driving point values. By neglecting higher order terms and rearranging one finds

$$I_{Na}(V_H, \Delta V) = \bar{I}(V_H) + \Delta I(V_H, \Delta V) \tag{6b}$$

with

$$\Delta I = \bar{P} \cdot (dI_0/dV) \cdot \Delta V + \bar{I}_0 \cdot (dP/dV) \cdot \Delta V. \tag{6c}$$

Differentiation with respect to V yields

$$\Delta I/\Delta V = \bar{P} \cdot (dI_0/dV) + \bar{I}_0 \times (dP/dV). \tag{6d}$$

On the right side only P is time-dependent [Eq. (1c)], since I_0 responds instantaneously to dV, making dI_0/dV just like $\bar{P}$ and $\bar{I}_0$ a constant at any given V_H. Therefore the admittance of the relaxation process is

$$Y_r = \bar{P} \cdot (dI_0/dV) + \bar{I}_0 \cdot (dP/dV)^* \tag{7}$$

with the star denoting a transform. Substitution with Eq. (1d) yields

$$Y_r = \bar{P} \cdot dI_0/dV + \bar{I}_0 \cdot d\bar{P}/dV \cdot (1/(1 + s/\lambda)). \tag{7a}$$

With the abbreviations

$$G_1 = \bar{P} \cdot dI_0/dV$$
$$\Delta G = \bar{I}_0 \cdot d\bar{P}/dV$$
$$L = \Delta G^{-1} \cdot \lambda^{-1}$$

defining the elements of the equivalent network of Fig. 3B, we obtain after substitution of s by $j\omega$

$$Y_r = G_1 + \frac{\Delta G}{1 + \omega^2/\lambda^2} + j \frac{-\Delta G \cdot \omega/\lambda}{1 + \omega^2/\lambda^2}$$

and therefore by rationalization

$$|Y_r| = \left(\frac{(G_1 + \Delta G)^2 + G_1^2 \cdot \omega^2/\lambda^2}{1 + \omega^2/\lambda^2} \right)^{1/2}. \tag{7b}$$

The characteristic relaxation rate λ is found at

$$|Y_r|_{\omega = 2} = 0.707 \cdot G_1 \cdot [1 + (1 + \Delta G/G_1)^2]^{0.5}.$$

Equation (7b) predicts that the magnitude of Y_r will approach G_1 at high frequencies and $G_1 + \Delta G$ at low frequencies. If $d\bar{P}/dV$ and therefore ΔG is negative, the low-frequency value will be smaller than the high-frequency value, in agreement with our data (Fig. 3A).

It remains to understand ΔG or rather $d\bar{P}/dV$ in terms of the rate constants. Combining Eqs. (2) and (3) we find

$$\bar{P} = k_{\text{off}}(V)/\lambda(V) \tag{2a}$$

and by differentiation

$$d\bar{P}/dV = \lambda^{-2} \cdot (\lambda \cdot dk_{\text{off}}/dV - k_{\text{off}} \cdot d\lambda/dV). \tag{8}$$

Therefore

$$G_1 = (k_{\text{off}}/\lambda) \cdot dI_0/dV \tag{9}$$

$$\Delta G = \bar{I}_0[(1/\lambda) \cdot (dk_{\text{off}}/dV) - (k_{\text{off}}/\lambda^2) \cdot (d\lambda/dV)] \tag{10}$$

or, after substitution of $\bar{I}_0$ with Eq. (6a),

$$\Delta G = \bar{I}_{Na} \left[\frac{1}{k_{\text{off}}} \cdot \left(\frac{dk_{\text{off}}}{dV} \right) - \frac{1}{\lambda} \cdot \left(\frac{d\lambda}{dV} \right) \right]. \tag{10a}$$

Following Cuthbert's blocking model [8], we shall suppose that the positively charged amidino
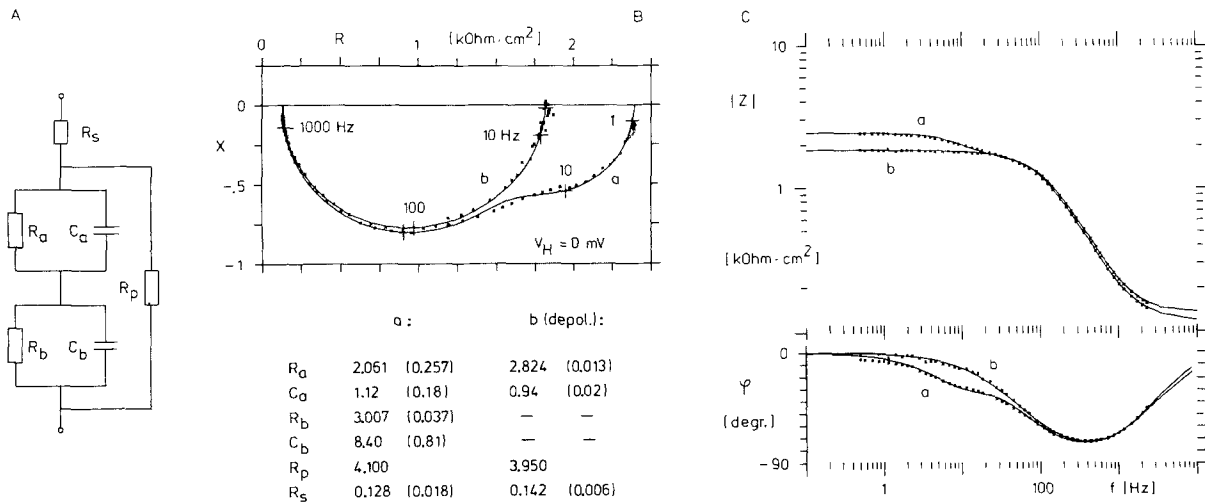
Fig. 1. (A) Electrical equivalent network (minimal complexity) of an epithelium (one cell layer) with a paracellular diffusion pathway of resistance R_p. The apical membrane is represented by its slope resistance and capacitance (R_a, C_a) and placed in series to R_b, C_b of the basolateral membrane, R_s is that part of the solution series resistance which, as the product with the current flowing, contributes to the voltage measurement in the four electrode voltage-clamp circuit. For the representation of additional relaxation components see Fig. 3B. (B) Nyquist diagram of the epithelial impedance corresponding to 1 cm² of chamber aperture. The real component of Z is plotted versus the imaginary component X. The mucosal solution was Na_2SO_4-Ringer's of 60 mM Na activity, pH 5.5, for both (a) and (b). The holding voltage was 0 mV. (a): NaCl-Ringer's on the serosal side. (b): 30 min after onset of the K-depolarization, which was affected by replacing the serosal NaCl-Ringer's with a KCl-sucrose solution [31]. The solid curves indicate best fits based on the structural model of panel A. Imperfections of the fit near 1 Hz were caused by parameter drift. The relative mean error was 0.026 for (a) and 0.036 for (b). (C) Bode diagram of the data of panel B. The circuit component values indicated on the left were obtained by nonlinear regression (drawn-out curves) and are given in kΩ cm² and μF/cm² of chamber aperture. Values in brackets are 95% confidence limits. Prior to depolarization R_b was found to be surprisingly large relative to R_a. The value may be misleading because curve a of panel B indicates that the structural model used for the basolateral membrane lacks complexity. This problem awaits further experimentation
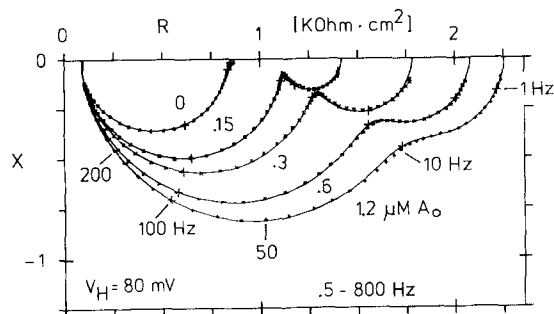

Fig. 2. Nyquist diagram of the impedance of a K-depolarized epithelium exposed to 60 mM Na_o. Addition of submaximal concentrations of amiloride to the mucosal solution increased the apical resistance and, at the same time, generated an additional dispersion at low frequencies (relaxation component, half circles on the right). The apical capacitance C_a remained unaffected at values near 1 μF/cm² of chamber aperture

group of amiloride dips into the channel entrance during each blocking event. Then the voltage dependence of the overall rate constants takes the form

$$k_{on}(V) = k_{on}^0 \exp(+\delta_{on} \cdot V/(RT/F)) \qquad (11)$$

$$k_{off}(V) = k_{off}^0 \exp(-\delta_{off} \cdot V/(RT/F)) \qquad (12)$$

where δ_{on} and δ_{off} indicate the dimensionless fractions of V sensed by the amidino group during a

single-step encounter and release, multiplied with the effective charge on this group. The superscript "0" designates zero mV. R, T and F have their usual meaning. With

$$\delta_s = \delta_{on} + \delta_{off}$$

we obtain

$$K_A(V) = (k_{off}^0/k_{on}^0) \exp(-\delta_s \cdot V/(RT/F)) \qquad (3a)$$

showing that K_A will decrease, i.e. more channels will be blocked, when V is made more positive. Returning to Eq. (10a), it is obvious now that dk_{off}/dV will be negative, while $d\lambda/dV$ will be positive at large A_o but negative at low A_o. Therefore negative values of ΔG (Fig. 3) are quite compatible with theory.

Results

IMPEDANCE AND K DEPOLARIZATION

For two series membranes of different time constants one expects a double dispersion in the impedance spectrum. Indeed, with Na_2SO_4 Ringer's on the mucosal and NaCl Ringer's on the serosal side,
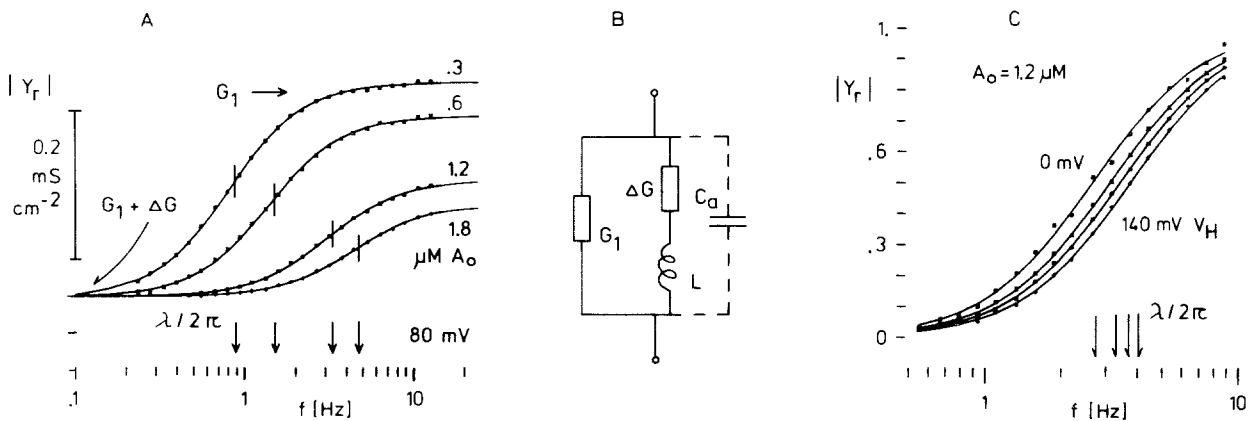
Fig. 3. (A) After converting impedance to admittance, the capacitive component C_a was subtracted. The remaining relaxation admittance Y_r is plotted as magnitude (linear scale) versus frequency (log scale). Equation (7b) was fitted to the data points by nonlinear regression, yielding parameter values for G_1, ΔG and λ (see panel B). Subsequently the curves were shifted along the ordinate such that their low-frequency asymptotes coincide. Both G_1 and the magnitude of ΔG decrease when A_o is raised, while λ increases with A_o. (B) Equivalent network of the A_o-dependent relaxation process. The apical membrane slope conductance G_a is modeled as a frequency independent term G_1 [Eq. (9)] plus a voltage-dependent negative quantity ΔG [Eq. (10a)]. (C) Relaxation admittance spectra were obtained at holding voltages of 0, 60, 100 and 140 mV and normalized to equal low- and high-frequency asymptotes, to show the voltage dependence of λ more clearly. Curve fitting as described for panel A

the spectrum of the epithelium of toad urinary bladder often shows this double dispersion (Fig. 1B and C, curves labeled a). From it the circuit parameters of Fig. 1A may be calculated after determination of the shunt resistance R_p in the presence of 30 μM amiloride. 30 min after replacing the serosal solution with the depolarizing KCl-sucrose medium [31] R_b was found to be decreased from 3.0 to less than 0.1 kΩ cm². In consequence, the impedance was now dominated by that of the apical membrane (curves labeled b in Fig. 1), which was increased by the depolarization. This increase will, to a large extent, be due to an increase in the slope resistance R_a as expected from the shape of the apical $I_{Na}(V)$ curve [12, 16, 31]. R_s increased slightly due to the lower ion content of the KCl-sucrose solution. R_p was little affected.

In a few toad bladder preparations R_b was found to be in the order of 0.2 kΩ cm² prior to K depolarization. In these cases the depolarization had a less dramatic effect on R_b.

IMPEDANCE EFFECT OF SMALL AMILORIDE CONCENTRATIONS

When amiloride was added in submaximal concentrations to the mucosal solution (60 mM Na_o) of K-depolarized epithelia, the resistance increased as expected. At the same time a new discrete dispersion appeared at low frequencies. It is particularly evident at mucosally positive holding voltages as shown in the Nyquist diagram of Fig. 2, which was obtained at $V_H = +80$ mV. The characteristic frequency of this new dispersion increases systematically with the amiloride concentration (Eq. 4). Fur-

thermore, the characteristic frequency is much larger when the same level of blockage is achieved with triamterene rather than amiloride. As triamterene has a higher blocking rate (e.g. 20), this finding indicates that the dispersion arises from a voltage-dependent relaxation property of the apical membrane and is not, for instance, due to the reappearance of R_b. This conclusion is further supported by the unreasonably high values of C_b of more than 100 μF/cm² of chamber aperture which are computed if the dispersion is treated as arising from an R_b, C_b-element.

THE RELAXATION COMPONENT IN ADMITTANCE SPECTRA

In order to study the amiloride-dependent relaxation in detail, the apical impedance was converted to admittance and the additive component

$$Y_c = j\omega C_a$$

due to the membrane capacitance subtracted. The remainder is the relaxation admittance Y_r which was analyzed in terms of the equivalent network of Fig. 3B. Examples are given in Fig. 3A. Note that the sigmoid data curves were shifted to different extents along the ordinate to make the change of ΔG with increasing A_o more clearly noticeable. Equation (7b) was fitted to these data by nonlinear regression (drawn-out curves), yielding the parameters G_1, ΔG and λ (with ΔG of negative values) and their 95% confidence limits. It is apparent that λ increases with A_o (arrows in Fig. 3A) as well as with the holding voltage (arrows in Fig. 3C). The theoret-
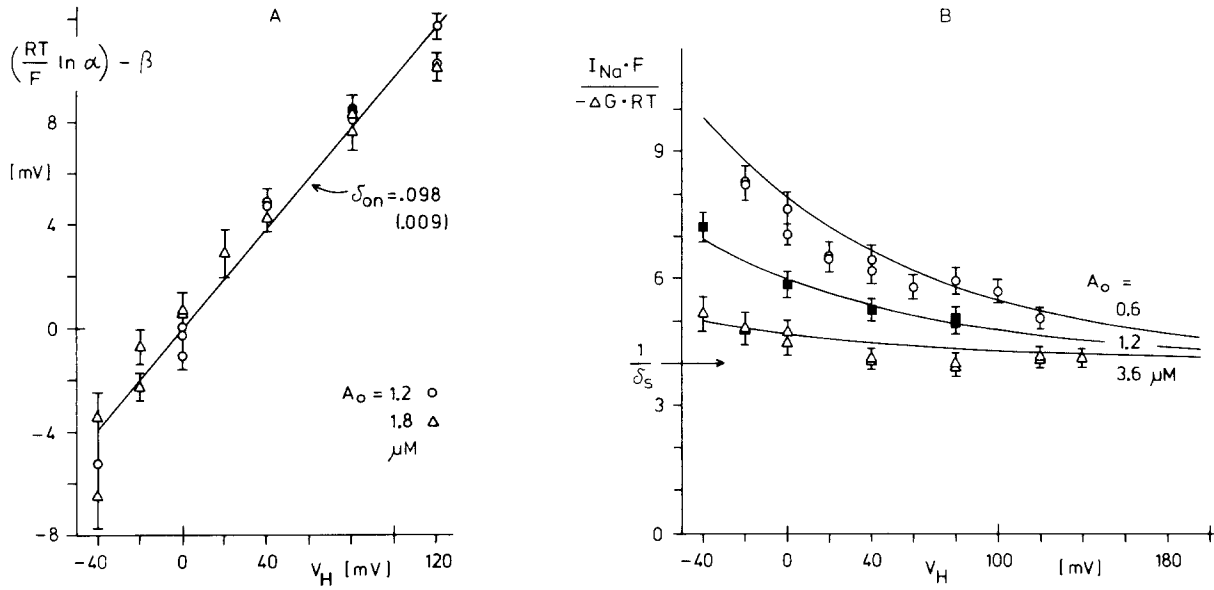
Fig. 4. (A) Determination of δ_{on} (mode A). Data obtained at two amiloride concentrations were converted to $(RT/F) \ln(-\Delta G \cdot \lambda/\bar{I}_{Na})$ and plotted against the holding voltage used. The error bars shown indicate 95% confidence limits. Weight factors were used in fitting. Linear regression retrieved $\delta_{on} = 0.098 + 0.005$ (SD) as the slope (the 95% confidence limit would be twice as large as the SD) and β as given by Eq. (10c). For display purposes β was then subtracted from the ordinate values. (B) Determination of δ_s (mode A). Data obtained at three A_o as indicated were converted to the dimensionless ratio $-\bar{I}_{Na}/(\Delta G \cdot RT/F)$ (with ΔG being negative) and plotted against the holding voltage used. The error bars shown indicate 95% confidence limits. Weight factors were used in fitting. Equation (10d) was fitted *jointly* to the three sets of data, yielding $\delta_s = 0.248$ (0.022, 95% confidence limit) as the asymptotic value at high V_H and $K_A^0 = 0.57$ (0.18) μM

ical meaning of G_1, ΔG and λ is given by Eqs. (9), (10) and (4) in conjunction with Eqs. (11) and (12).

DETERMINATION OF δ_{on} (MODE A)

Rearrangement of Eq. (10a) yields

$$\frac{-\Delta G}{\bar{I}_{Na}} = \frac{1}{\lambda} \cdot \left(\frac{d\lambda}{dV}\right) - \frac{1}{k_{off}} \cdot \left(\frac{dk_{off}}{dV}\right). \tag{10b}$$

After differentiation of Eqs. (4) and (12), insertion into Eq. (10b) and further rearrangement we obtain

$$(RT/F) \ln \alpha = \beta + \delta_{on} \cdot V_H \tag{10c}$$

with

$$\alpha = -\Delta G \cdot \lambda/\bar{I}_{Na}$$
$$\beta = (RT/F) \cdot \ln(k_{on}^0 \cdot A_o \cdot \delta_s/(RT/F)).$$

Thus a plot of $(RT/F) \ln \alpha$ versus V_H is expected to yield a straight line of slope δ_{on}. Examples are shown in Fig. 4A. From such plots, δ_{on} was determined by linear regression for each amiloride concentration used. Note that this procedure makes use of both amplitude $(\Delta G, \bar{I}_{Na})$ and rate information

(λ). The estimated δ_{on} values are compiled in Fig. 5A, plotted versus A_o. The slope of the regression line is not significantly different from zero.

DETERMINATION OF δ_s (MODE A)

By taking the inverse of Eq. (10b) we obtain

$$\frac{\bar{I}_{Na}}{-\Delta G \ RT/F}$$
$$= \frac{A_o k_{on}^0 \exp \dfrac{\delta_{on} \cdot V}{RT/F} + k_{off}^0 \exp \dfrac{-\delta_{off} \cdot V}{RT/F}}{k_{on}^0 \cdot A_o \cdot \delta_s \exp(\delta_{on} \cdot V/(RT/F))}$$

which simplifies to

$$\frac{\bar{I}_{Na}}{-\Delta G \cdot RT/F} = \frac{1}{\delta_s} + \frac{\exp - \delta_s \cdot V/(RT/F)}{\delta_s \cdot A_o/K_A^0}. \tag{10d}$$

For plots of the left-hand side of this equation versus V_H we expect a decaying exponential which approaches $1/\delta_s$ at high V_H, as shown in Fig. 4B. By fitting Eq. (10d) to these data, the parameters δ_s and (with less accuracy) K_A^0 were retrieved by nonlinear regression, together with their 95% confidence lim-
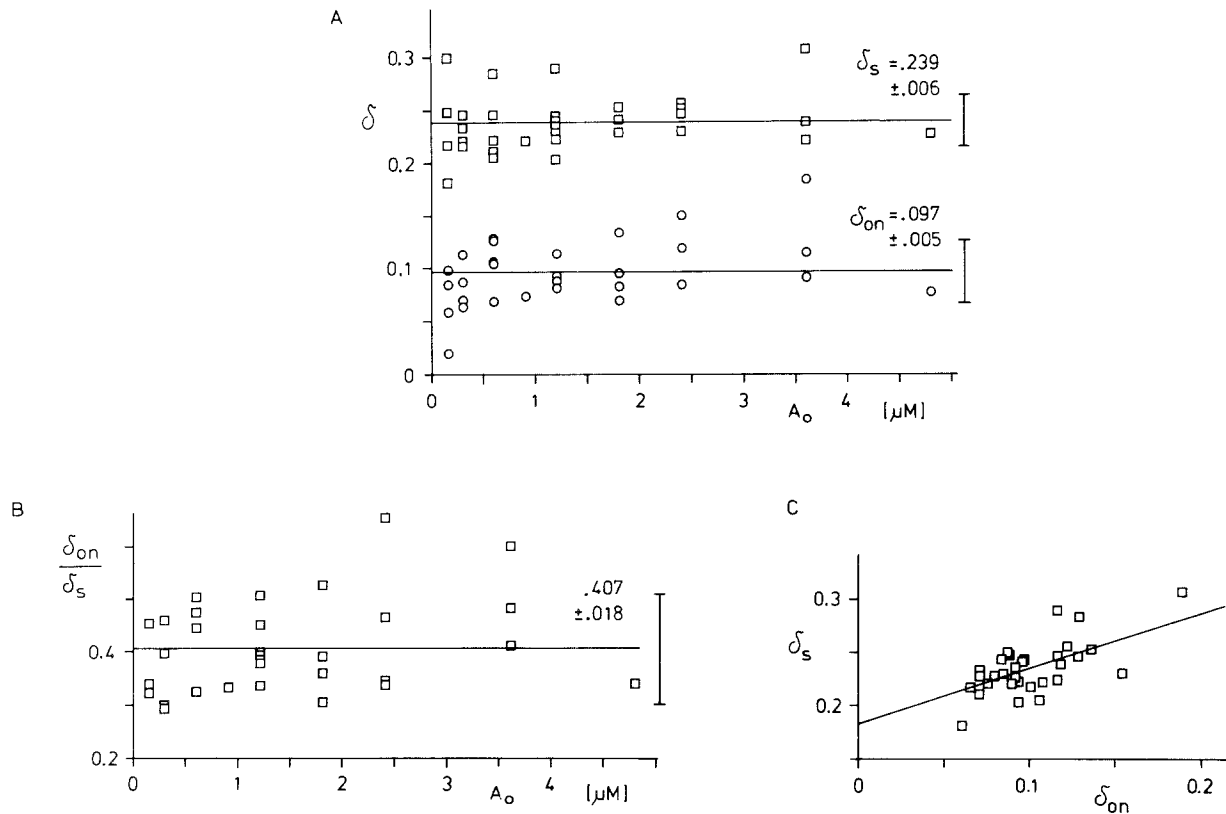
Fig. 5. (A) Compilation of 34 δ_s and δ_{on} values (obtained by mode A from seven preparations), plotted against the amiloride concentration used in their determination. Calculated regression lines have slopes not significantly different from zero. The horizontal lines indicate the mean values (calculated *without* using weight factors of individual points). The standard errors of the mean (SEM), which are needed for the paired *t*-test, are printed on the right. The standard deviations are indicated by vertical bars. From these results, δ_{off} may be determined as $\delta_s - \delta_{on} = 0.142 \pm 0.038$ (SD). (B) Data of panel A. The ratio δ_{on}/δ_s has a mean value of 0.404 ± 0.014 (SEM) when weights are used in its calculation. Thus it is significantly smaller than 0.5. (C) Data of panel A. The regression line obeys the relationship $\sigma_s = 0.18 \pm 0.01 + (0.48 \pm 0.11) \cdot \delta_{on}$. Thus the estimated value of δ_s correlates weakly with that on δ_{on}

its. Note that this procedure does not require rate information. The values of δ_s thus obtained are compiled in Fig. 5A.

The mean values indicated in Fig. 5A were calculated without the use of weight factors obtained from the confidence limits of the δ values. When such weights are used, slightly different means result, as listed in the Table (mode A). δ_{off} was computed as $\delta_s - \delta_{on}$. The *t*-test was applied to the 34 δ_{on}, δ_{off}-pairs and yielded a *t*-value >5. Therefore the mean δ_{off} is larger than the mean δ_{on} with a probability >0.99.

The procedures described above for the determination of δ_{on} and δ_s have the advantage that their accuracy does not depend on the prior, or simultaneous, estimation of *rate constant* values. This is possible because rate information is either mixed with amplitude information or not used at all. The disadvantage is that amplitude errors become critical. Particularly the seemingly trivial estimation of $\bar{I}_{Na}$, which requires the subtraction of the not ami-

loride blockable shunt current, can be erroneous for various reasons [e.g. 22]. This probably explains the scatter of δ values in Fig. 5A and the slight dependence of δ_s on δ_{on} shown in Fig. 5C.

DETERMINATION OF RATE CONSTANTS (MODE A OR B)

λ values, obtained as shown in Fig. 3A, were plotted against the holding voltage, using the amiloride concentrations as parameters. Figure 6 gives two examples out of seven evaluated experiments. Differentiation of Eq. (4) [in conjunction with Eqs. (11) and (12)] shows that the $\lambda(V)$ relationship should have a minimum at the voltage

$$-(RT/F) \cdot \delta_s \ln \frac{A_o \cdot \delta_{on}}{K_A^0 \cdot \delta_{off}}.$$

The minimum will become more shallow and shift

Table. δ values and global blocking rate constants of amiloride obtained from admittance spectra, using mixed amplitude and rate information (mode A) or merely rate information (mode B)[a]

Mode/ref.	δ_s	δ_{on}	δ_{off}	k_{on}^0	k_{off}^0	weights	n
A	0.239	0.097	0.142	9.77	3.02	—	34
	±0.025	±0.028	±0.038	±0.98	±0.84		
A	0.234	0.095	0.139	9.73	2.92	yes	34
	±0.017	±0.019	±0.025	±0.87	±0.82		
B	0.281	0.108	0.173	9.41	3.23	—	7
	±0.065	±0.021	±0.062	±1.21	±0.72		
B	0.213	0.100	0.113	9.41	2.85	yes	7
	±0.034	±0.017	±0.029	±0.80	±0.76		
TB[30]	0.150			9.6	2.26		6
	±0.025						
TB[21]				17.90	2.66		9
				±1.98	±2.40		
FS[20]				13.17	3.93		58
				±1.88	±1.47		

[a] Based on 274 values of ΔG and δ from 7 toad bladder preparations exposed to 60 mM Na_o. Values from the literature are given for comparison. Rate constants are in sec $^{-1}$ μM $^{-1}$ and in sec $^{-1}$. Values are given ±SD. "Yes" indicates that weights derived from 95% confidence limits were used for averaging. TB: toad urinary bladder; FS: frog skin.
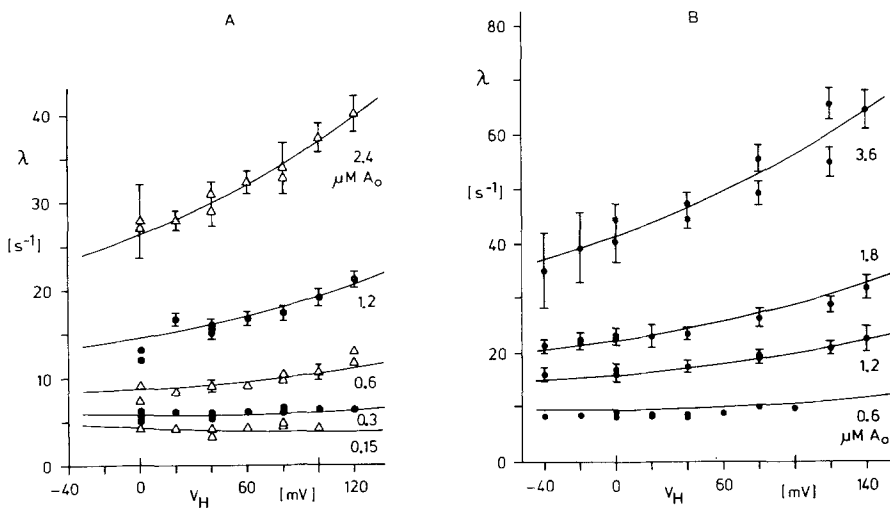

Fig. 6. λ values and their 95% confidence limits (bars) were retrieved from $|Y_r|$ as shown in Fig. 3A and plotted against the holding voltage. Two experiments out of seven. The curved lines were obtained by fitting Eq. (4) *jointly* to all data points of one panel, yielding k_{on}^0, k_{off}^0, δ_{on} and δ_{off} and their 95% confidence limits (mode *B*, see Table). For the fit, weight factors of individual λ values, calculated from their confidence limits, were used

to more positive voltages when A_o is lowered, as the data of Fig. 6 appear to indicate. Most of our data points are on the right branch of the $\lambda(V)$ relationship shown. Equation (4) indicates they will at high A_o estimate k_{on} better than k_{off} while at low A_o the opposite is true. Therefore it is important that a fit with Eq. (4) is applied *jointly* to the data obtained at high and low A_o.

The data points of each single panel (*see* Fig. 6) were jointly fitted with Eq. (4) [in conjunction with Eqs. (11) and (12)]. The fit used weight factors of λ values, calculated from 95% confidence limits. For this purpose confidence limits smaller than 0.1 sec^{-1} were set equal to 0.1 sec^{-1}. In *mode A* the mean

values already obtained for δ_{on} and δ_{off} (Table) were used as constants in the fit such that only k_{on}^0 and k_{off}^0 had to be retrieved.

In *mode B* δ values were not specified as constants but retrieved as fit parameters. This procedure, then, does not use amplitude information at all. Each joint fit (two examples are given in Fig. 6) yielded values for δ_{on}, δ_{off}, k_{on}^0 and k_{off}^0 and their 95% confidence limits. The mean parameter values found in mode B are also listed in the Table. The δ values are in reasonable agreement with those obtained by the mixed amplitude and rate procedure (mode A). Again δ_{off} appears to be somewhat larger than δ_{on}.
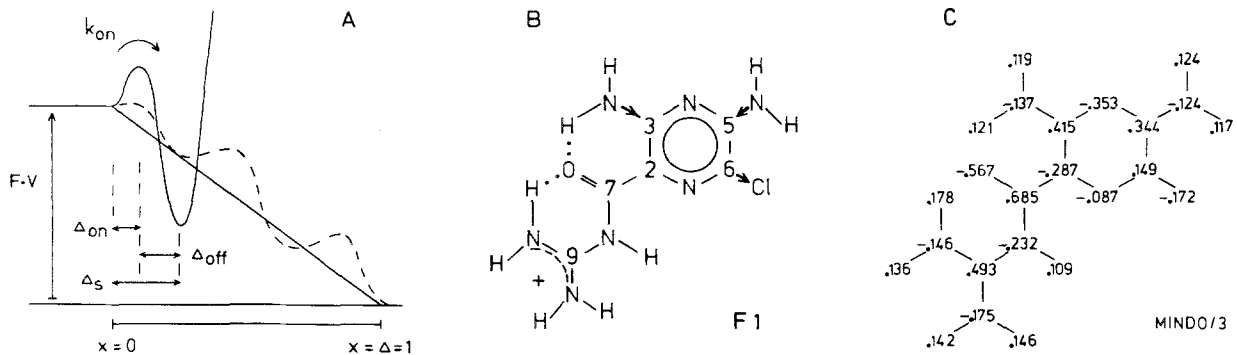
Fig. 7. (A) Schematic profile of activation energies [9, 33] for diffusion of a Na ion through the apical channel (dashed curve) and for invasion of the channel entrance by amiloride or part of the amiloride molecule (drawn-out curve, compare [19]). The mucosal side (on the left) has been given a positive voltage with respect to the cytosol. The geometry parameters Δ_{on}, Δ_{off} and Δ_s are fractions of Δ as indicated by the length of the four horizontal lines. (B) Structure of the positively charged form of amiloride. Shown is the F1-conformer of Smith et al. [36]. According to their semiempirical calculations (using CNDO/2) F1 is the most likely charged state in the gas phase. Probably it is the dominant state in free aqueous solution of pH 7 and below, characterized by an almost ideally planar arrangement of atoms in pyrazine ring and side chain due to two intramolecular hydrogen bonds at the carbonyl oxygen. The arrows at pyrazine ring position -3, -5 and -6 point in the direction in which electrons are displaced by the ligand. Those pointing towards the ring indicate electropositive, those pointing away electronegative ligands compared to hydrogen. (C) Charge distribution on the protonated F1-conformer as calculated with MINDO/3 (disregarding solvation effects). The added charge on atoms of the terminal amidino group is estimated to $+0.77$, that of the guanidinium group to $+0.65$. For the deprotonated molecule (A1 of ref. [36]) the values are $+0.48$ (amidin-) and -0.03 (guanidin-residue). The program estimated the normal enthalpy of formation of F1 to $\Delta H_f^0 = +45$ and that of A1 to -81 kcal mol $^{-1}$

Discussion

In the past, noise analysis was used in numerous studies to determine the "global" blocking rate constants k_{on} and k_{off} of amiloride (for reviews see [22, 23]). In the present study we show that, by virtue of the newly discovered voltage dependence of these rate constants [14, 16, 29], their values can also be obtained in macroscopic experiments, in this case from admittance data. The k_{off}^0 value found is in reasonable agreement with that obtained by noise analysis in frog skin [e.g., 19, 20, 24] and toad bladder [21], considering the standard deviations listed in the Table. The k_{on}^0 value found at 60 mM Na$_o$ is reasonably close to that obtained by noise analysis in frog skin at the same Na$_o$ [e.g. 19] but significantly smaller than that found with toad bladder at 60 mM Na$_o$ but a different mucosal pH [21]. The values found by Palmer for toad bladder, using a pulse relaxation technique [30], are again in agreement with ours.

The equations used for analysis were derived with a special molecular model in mind: As previously proposed by Cuthbert [8], the protonated amiloride or a positively charged part of this molecule occupies the channel entrance during blockage. When supposing that the on- and off-process can be approximately described by single-step kinetics (probably an idealization), then δ_{on} and δ_{off} are mea-

sures of the dimensionless fraction of membrane voltage sensed by this mobile positive charge during onset and termination of block period [Eqs. (11) and (12)]. The concept is best explained in terms of Eyring rate theory [e.g. 9, 33]. In Fig. 7A the dashed curve depicts schematically the profile of Gibbs free energy of activation for the passage of a Na ion through the channel. The two dominant barriers are on the right. One of them would be the selectivity filter. The membrane voltage is shown as mucosal side positive with respect to cytosol, and the superimposed electrical field dV/dx is constant, i.e., voltage drops linearly along the diffusion pathway. The drawn-out curve depicts schematically the energy profile for binding of amiloride to the channel entrance (see [19]). The left barrier on this profile will be called access barrier. With the channel length Δ normalized to unity, Δ_s is the fractional distance from free solution to the energy well of the blocking position. Δ_{on} will be the dimensionless fraction of V sensed by a charge which overcomes the access barrier from the left with a single reaction step. Suppose the charge moved is of the value z_{on} during encounter but of value z_{off} during release. Then

$$\delta_{on} = z_{on} \cdot \Delta_{on}$$

$$\delta_{off} = z_{off} \cdot \Delta_{off}$$

$$\delta_s = z_{on} \cdot \Delta_{on} + z_{off} \cdot \Delta_{off} \tag{13}$$

are the quantities used in Eqs. (3a), (11) and (12). If the channel is free of other displacable charges, z_{on} and z_{off} will refer to the charge of the invading group. For a number of reasons δ_{on} and δ_{off} need not be identical. Firstly, the access barrier may be asymmetrical. Secondly, the applied electrical field may not be constant along x. Third, the voltage drop across the access barrier may become larger while the channel is blocked. In each of these cases $\Delta_{on} \neq \Delta_{off}$ will result. Fourth, the mobile charge may change. Suppose only the amidino group of amiloride invades the channel entrance. Its net positive charge may increase for the time in which the chlorine atom at position-6 of the pyrazine ring interacts with an electropositive residue of the receptor [19], withdrawing negative charge from the side chain.[1] Then $z_{off} > z_{on}$ would result. In view of these possibilities[2] it is almost surprising to find δ_{off} only slightly larger than δ_{on}. The paired t-test shows that the mean values are different with a probability of >0.99.

The total charge on the protonated amiloride molecule is, of course, +1. However, if for steric reasons only the side chain can occupy the channel entrance, we will have to know the charge on this part of the molecule. Based on the selfconsistent-field molecular orbital approach, Mrs. C. Dorweiler estimated the charge distribution on the protonated amiloride semiempirically. The standard MINDO/3 program [6] was applied to configuration F1 [36]. Three parameters of equilibrium geometry (i.e. bond length, bond angles, dihedral angles) were optimized with the Davidon-Fletcher-Powell algorithm [10] to find the minimum of total molecular energy. The result (Fig. 7C) shows the added charge on atoms of the amidino group to be in the order of +0.77. When using this value for z_{on} and z_{off}, we estimate that the center of this charge occupies a blocking position at an electrical distance of about 30% of membrane voltage away from the outer membrane surface. The selectivity filter, then, will be at an even deeper location. In reality the charge on the amidino group is obviously not a point charge, and the concepts used in conjunction with Fig. 7A are idealizations in several respects. We want to stress, however, that the charge is smaller than +1.

That the apical amiloride-blockable Na translo-

cators are channels was originally inferred from fluctuation analysis [24]. Support came from estimations of the flux ratio exponent [2, 28] and more recently from results with patch-clamp techniques [14] as well as with reconstituted membrane material [27, 34][3]. In spite of numerous investigations the blocking mechanism of amiloride at the epithelial Na channels has remained controversial. The issue is complicated by the possibility that the channels of the different amphibian species investigated may have differently located amiloride receptors [1, 3, 4]. Furthermore, in some tissues the channels may have more than one such receptor [5]. Our results with toad urinary bladder exposed to 60 mM Na_o appear compatible with a plug-type blocking model, as originally proposed by Cuthbert [8]. The recent results of Palmer [29, 30] are also compatible with this model, i.e. that the amidino group occludes the channel entrance during blockage. Interaction of the amidino group with a carboxyl group of the channel entrance [32, 41] could stabilize the blocking position together with binding of the 6-Cl atom to a receptor location at the periphery of the entrance [19]. The model may be checked further by investigating the voltage dependence of competition between amiloride and the transported Na ion [11, 25, 30] at different Na concentrations.

References

1. Benos, D.J. 1982. Amiloride: A molecular probe of sodium transport in tissues and cells. *Am. J. Physiol.* **242**:C131–C145

---

[1] Our MINDO/3 calculations have shown that changes in the electronegativity of the 6-ligand (e.g. substitution of Cl by H) will *not* affect the charge on the amidino group. However, such calculations apply to molecules *in the gas phase* and neglect solvation effects. In aqueous solution amiloride responds with a pronounced increase of pK_a to a substitution of 6-Cl by 6-H (*see* Table 1 in [19]).

[2] The effect of A_o-competitors like Na and K ions [e.g. 11, 25, 30] on k_{on} and δ_{on} will be discussed in a subsequent paper (Warncke & Lindemann, *in preparation*).

---

[3] Na channel patch-clamp records from the apical membranes of aldosterone-stimulated A6-cell cultures show the expected flickering of the current trace when amiloride is present at the outer membrane surface in submaximal concentrations [14]. In contrast, Na channels in membrane vesicles from A6-cells, when fused into decane-containing planar lipid bilayers, do not show this flickering below 100 Hz [34]. However, A_o-induced current flickering may occur at unexpectedly high rates in this system. It appears desirable to record A_o-induced current noise or admittance components from confluent A6-cell layers in order to learn how the Na channels are altered by the reconstitution procedure.

2. Benos, D.J., Hyde, B.A., Latorre, R. 1983. Sodium flux ratio through the amiloride-sensitive entry pathway in frog skin. J. Gen. Physiol. 81:667–685

3. Benos, D.J., Mandel, L.J., Balaban, R.S. 1979. On the mechanism of the amiloride-sodium entry site interaction in anuran skin epithelia. J. Gen. Physiol. 73:307–326

4. Benos, D.J., Mandel, L.F., Simon, S.A. 1980. Effects of chemical group specific reagents on sodium entry and the amiloride binding site in frog skin: Evidence for separate sites. J. Membrane Biol. 56:149–158

5. Benos, D.J., Watthey, J.W.H. 1981. Inferences on the nature of the apical sodium entry site in frog skin epithelium. J. Pharmacol. Exp. Ther. 219:481–488

6. Binghma, R.C., Dewar, M.J.S., Lo, D.H. 1975. Ground states of molecules. XXV. MINDO/3. An improved version of the MINDO semiempirical SCF-MO method. J. Am. Chem. Soc. 97:1285–1293

7. Clausen, C., Lewis, S.A., Diamond, J.M. 1979. Impedance analysis of a tight epithelium using a distributed resistance model. Biophys. J. 26:291–318

8. Cuthbert, A.W. 1976. Importance a guanidinium groups for blocking sodium channels in epithelia. Mol. Pharmacol. 12:945–957

9. Eyring, H., Lumry, R., Woodbury, J.W. 1949. Some applications of modern rate theory to physiological systems. Rec. Chem. Prog. 10:100–114

10. Fletcher, R., Powell, M.J.D. 1963. A rapidly convergent descent method for minimization. Computer J. 6:163–168

11. Frehland, E., Hoshiko, T., Machlup, S. 1983. Competitive blocking of apical sodium channels in epithelia. Biochim. Biophys. Acta 732:636–646

12. Fuchs, W., Hviid Larsen, E., Lindemann, B. 1977. Current voltage curve of sodium channels and concentration dependence of sodium permeability in frog skin. J. Physiol. (London) 267:137–166

13. Gögelein, H., Van Driessche, W. 1981. Capacitive and inductive low frequency impedances of Necturus gallbladder epithelium. Pfluegers Arch. 389:105–113

14. Hamilton, K.L., Eaton, D.C. 1984. Single channel conductance events from the amiloride-sensitive Na conductance of epithelial cells. Fed. Proc. 43:628

15. Hansen, U.-P., Tittor, J., Gradmann, D. 1983. Interpretation of current-voltage relationships for "active" ion transport systems: II. Nonsteady-state reaction-kinetic analysis of Class-I mechanisms with one slow time-constant. J. Membrane Biol. 75:141–169

16. Henrich, M., Lindemann, B. 1984. Voltage dependence of channel currents and of channel densities in the apical membrane of toad urinary bladder. In: Intestinal Absorption and Secretion. E. Skadhauge and K. Heintze, editors. pp. 209–220. MTP, Lancaster

17. Kottra, G., Frömter, E. 1984. Rapid determination of intraepithelial resistance barriers by alternating current spectroscopy. I. Experimental procedures. Pfluegers Arch. 402:409–420

18. Kottra, G., Frömter, E. 1984. Rapid determination of intraepithelial resistance barriers by alternating current spectroscopy. II. Test of model circuits and quantification of results. Pfluegers Arch. 402:421–432

19. Li, J.H.-Y., Cragoe, E.J., Jr., Lindemann, B. 1985. Structure-activity relationship of amiloride analogs as blockers of epithelial Na channels. I. Pyrazine-ring modifications. J. Membrane Biol. 83:45–56

20. Li, J.H.-Y., Lindemann, B. 1983. Competitive blocking of epithelial sodium channels by organic cations: The relationship between macroscopic and microscopic inhibition constants. J. Membrane Biol. 76:235–251

21. Li, J.H.-Y., Palmer, L.G., Edelman, I.S., Lindemann, B. 1982. The role of sodium-channel density in the natriferic response of the toad urinary bladder to an antidiuretic hormone. J. Membrane Biol. 64:77–89

22. Lindemann, B. 1980. The beginning of fluctuation analysis of epithelial ion transport. J. Membrane Biol. 54:1–11

23. Lindemann, B. 1984. Fluctuation analysis of sodium channels in epithelia. Annu. Rev. Physiol. 46:497–515

24. Lindemann, B., Van Driessche, W. 1977. Sodium specific membrane channels of frog skin are pores: Current fluctuations reveal high turnover. Science 195:292–294

25. Lindemann, B., Warncke, J. 1985. Dependence of the blocking rate constants of amiloride on the mucosal Na concentration. Pfluegers Arch. 403:R13

26. Mauro, A., Conti, F., Dodge, F., Schor, R. 1970. Subthreshold behavior and phenomenological impedance of the squid giant axon. J. Gen. Physiol. 55:497–523

27. Olans, L., Sariban-Sohraby, S., Benos, D.J. 1984. Saturation behavior of single amiloride-sensitive Na channels in planar lipid bilayers. Biophys. J. 46:831–835

28. Palmer, L.G. 1982. Na transport and flux ratio through apical Na channels in toad bladder. Nature (London) 297:688–690

29. Palmer, L.G. 1984. Voltage-dependent block by amiloride and other monovalent cations of apical Na channels in the toad urinary bladder. J. Membrane Biol. 80:153–165

30. Palmer, L.G. 1985. Interactions of amiloride and other blocking cations with the apical Na channel in the toad urinary bladder. J. Membrane Biol. (in press)

31. Palmer, L.G., Edelman, I.S., Lindemann, B. 1980. Current-voltage analysis of apical sodium transport in toad urinary bladder: Effects of inhibitors of transport and metabolism. J. Membrane Biol. 57:59–71

32. Park, C.S., Kipnowski, J., Fanestil, D.D. 1983. Role of carboxyl group in Na-entry at apical membrane of toad urinary bladder. Am. J. Physiol. 245:F707–F715

33. Parlin, B., Eyring, H. 1954. Membrane permeability and electrical potential. In: Ion Transport across Membranes. H.T. Clarke, editor. pp. 103–118. Academic, New York

34. Sariban-Sohraby, S., Latorre, R., Burg, M., Olans, L., Benos, D. 1984. Amiloride sensitive epithelial Na channels reconstituted into planar lipid bilayer membranes. Nature (London) 308:80–82

35. Smith, P.G. 1971. The low-frequency electrical impedance of the isolated frog skin. Acta Physiol. Scand. 81:355–366

36. Smith, R.L., Cochran, D.W., Gund, P., Cragoe, E.J., Jr. 1979. Proton, carbon-13, and nitrogen-15 nuclear magnetic resonance and CNDO/2 studies on the tautomerism and conformation of amiloride, a novel acylguanidine. J. Am. Chem. Soc. 101:191–201

37. Strobel, H. 1968. Systemanalyse mit determinierten Testsignalen. VEB-Verlag, Berlin

38. Tittor, J., Hansen, U.-P., Gradmann, D. 1983. Impedance of the electrogenic Cl⁻ pump in Acetabularia: Electrical frequency entrainments, voltage-sensitivity, and reaction kinetic interpretation. J. Membrane Biol. 75:129–139

39. Warncke, J., Lindemann, B. 1979. A sinewave-burst method to obtain impedance spectra of transporting epithelia during voltage clamp. Pfluegers Arch. 382:R12

40. Warncke, J., Lindemann, B. 1985. Voltage dependence of Na channel blockage by amiloride: Admittance relaxation spectra. Pfluegers Arch. 403:R13

41. Zeiske, W., Lindemann, B. 1975. Blockage of Na channels in frog skin by titration with protons and by chemical modification of COO⁻ groups. Pfluegers Arch. 355:R71